

# Biomedical Materials



## PAPER

# Production and characterization of a coconut oil incorporated gelatin-based film and its potential biomedical application

RECEIVED  
12 February 2022

ACCEPTED FOR PUBLICATION  
3 May 2022

PUBLISHED  
18 May 2022

Mehlika Karamanlioglu<sup>1,2,\*</sup> and Serap Yesilkir-Baydar<sup>1,2</sup>

<sup>1</sup> Faculty of Engineering and Architecture, Department of Biomedical Engineering, Istanbul Gelisim University, İstanbul 34310, Turkey

<sup>2</sup> Istanbul Gelisim University, Life Sciences and Biomedical Engineering Application and Research Center, İstanbul 34310, Turkey

\* Author to whom any correspondence should be addressed.

E-mail: [mkaramanlioglu@gelisim.edu.tr](mailto:mkaramanlioglu@gelisim.edu.tr)

**Keywords:** coconut oil, gelatin, wound healing, wound dressing

## Abstract

The influence of coconut oil (CO) on a gelatin-based film was investigated when used as a potential wound dressing material. There is limited study on CO in protein-based wound dressing materials. Therefore, in this study a self-supporting, continuous and homogenous CO incorporated gelatin-based film was formulated and obtained by solution casting method. The influence of CO on physicochemical and thermal properties of gelatin-based film was also determined. Moreover, the effect CO in gelatin films on cell viability and cell migration was analysed with a preliminary cell culture study. Homogenous dispersion of 10% (w/w) CO was obtained in films when 3% (v/w) Tween 80, a surfactant, was incorporated to 20% (w/w) plasticized gelatin film forming solution. Effect of CO on gelatin-based film was observed via phase separation by scanning electron microscopy analysis. Water uptake of gelatin film with no CO, GE film; and 10% (w/w) CO incorporated GE film, GE-CO, were 320% and 210%, respectively, after 3 h in water. Fourier transform infrared spectroscopy analysis showed triglyceride component of CO and increased hydrogen bonding between NH groups of gelatin in GE-CO films. Differential scanning calorimetry results suggested a more ordered structure of GE-CO film due to an increase in melt-like transition temperature and melting enthalpy of GE-CO film. CO content also increased cell viability, assessed by XTT assay since cell viability was approximately 100% when L929 cell culture was incubated with GE-CO of 5–100  $\mu\text{g ml}^{-1}$ . Moreover, GE-CO samples within 5–25  $\mu\text{g ml}^{-1}$  concentration range, increased proliferation of L929 cells since cell viability was significantly higher than the 100% viable cell culture control ( $P < 0.05$ ) which is also an indication of efficient healing. However, GE decreased viability of L929 cells significantly at 100–10  $\mu\text{g ml}^{-1}$  concentration range ( $P < 0.05$ ) and were toxic at concentrations of 100, 75 and 50  $\mu\text{g ml}^{-1}$  which decreased  $\sim 50\%$  of the viability of the cells. Scratch Assay to assess *in vitro* wound healing showed cell migration towards scratch after 24 h as an indication of wound healing only in GE-CO samples. This study showed that, CO could efficiently be added to gelatin-based films for preparation of a primary wound dressing biomaterial which is also demonstrated to have a promising wound healing effect for minor wounds.

## 1. Introduction

The use of biomaterials for therapeutic purposes has been increasing in the last few decades (Zaman *et al* 2011, Parvez *et al* 2012, Rajpaul 2015, Yousefi *et al* 2017, Hajialyani *et al* 2018, Akhavan-Kharazian and Izadi-Vasafi 2019, Alkekhia *et al* 2020, Cheng *et al*

2020, Makvandi *et al* 2020, Sierra-Sánchez *et al* 2020, Taheri *et al* 2020, Huang *et al* 2021, Ndlovu *et al* 2021, Wang *et al* 2021).

Biomaterials obtained from renewable sources are applied widely in medicine and bioengineering fields and are generally used for tissue regeneration purposes (Tanase and Spiridon 2014, Cheng *et al* 2020,

Indurkar *et al* 2021, Kim *et al* 2021, Wang *et al* 2021). Biomaterial based wound dressing materials were determined to enhance wound healing since they are analogues of protein and growth factors to stimulate healing (Matsuda *et al* 1993, Grzybowski *et al* 1997, Zaman *et al* 2011, Ndlovu *et al* 2021). Wound dressings can consist of several materials and primary wound dressing is the part that comes into contact with the wound (Vowden and Vowden 2017). Gelatin is a protein based biomaterial obtained from collagen that has previously been used as primary wound dressing material due to its biocompatibility, no toxicity, bio-adhesiveness and haemostatic effects (Montero *et al* 1999, Zaman *et al* 2011, Parvez *et al* 2012, Huang *et al* 2020, Ndlovu *et al* 2021, Suleman Ismail Abdalla *et al* 2021). Gelatin is usually combined with a plasticizer to improve its mechanical properties to be applied as wound dressing material (Sezer and Cevher 2011, Zaman *et al* 2011, Conzatti *et al* 2018).

In recent years natural products such as plant based therapeutic agents have been used in various treatments such as wound healing (Shilling *et al* 2013, Ismail *et al* 2014, 2018, Muktar *et al* 2018, Ambika and Nair 2019, Indurkar *et al* 2021).

Coconut oil (CO), a natural oil, is obtained from *Cocos nucifera* tree in Indonesia and India and virgin CO, having more health benefits, is extracted from fresh coconut meat under controlled temperature (Srivastava *et al* 2017, Vaughn *et al* 2018). CO is conventionally used in food and cosmetics industry, however, recently been used in medicine due to its antimicrobial, anti-inflammatory, antioxidant, scar removal and skin barrier effects (Shilling *et al* 2013, Ismail *et al* 2014, Muhammad Zulhelmi Muktar 2017, Muktar *et al* 2018, Vaughn *et al* 2018). Virgin CO contains triglycerides, diglycerides, monoglycerides and free fatty acids (Dayrit 2015). Lauric acid content of CO, which is a component of triglycerides, was determined to have antimicrobial and anti-inflammatory properties (Dayrit 2015, Peedikayil *et al* 2016). When used as a mouthwash, CO was shown to reduce dental plaque forming *Streptococcus mutans* as much as the most effective oral pathogen reducing chemical agent chlorhexidine (Peedikayil *et al* 2016). In another study, CO was shown to inhibit *Clostridium difficile* which causes intestinal disorders (Shilling *et al* 2013). Moreover, CO was shown to have other advantages such as moisturizing effect thus preventing atopic dermatitis (Verallo-Rowell *et al* 2008). It has skin barrier property that prevents entry of microorganisms and foreign substances such as allergens, etc (Nangia *et al* 2015, Vaughn *et al* 2018). Also, CO was shown to be noncytotoxic to human skin fibroblast cells (Ismail *et al* 2014). However, there is limited research on designing CO as a component in a protein-based biomaterial and examining its effects on wound

healing under *in vitro* conditions. Therefore, this study was conducted to prepare and characterize CO incorporated homogenous gelatin-based primary wound dressing materials for minor wounds and to investigate their wound healing effect with a preliminary study.

## 2. Materials and methods

### 2.1. Materials

Virgin CO and bovine gelatin powder were obtained from Lokman Hekim (Ankara, Turkey). Glycerol (98% reagent grade) was purchased from ISOLAB (Eschau, Germany). Commercial grade Tween 80 (polyoxyethylene (20) sorbitan mono-oleate) was obtained from Sigma (Eschau, Germany). The mouse fibroblast cell line, L929, was obtained from Department of Bioengineering at Yildiz Technical University, Turkey. All the chemicals used in cell culture studies were analytical grade. The 2,3-bis-(2-methoxy-4-nitro-5-sulphophenyl)-2H-tetrazolium-5-carboxanilide (XTT), paraformaldehyde and crystal violet dye were purchased from Merck (Darmstadt, Germany). Dulbecco's Modified Eagle Medium/Nutrient Mixture F-12 (DMEM-F12) containing 4.5 g l<sup>-1</sup> of glucose was purchased from Pan Biotech (Germany). Other chemicals used in cell culture studies including ethanol were obtained from Pan Biotech (Germany), Neofroxx/BioFroxx (Germany), Sigma-Aldrich/Merck (USA), and CAPP (Denmark).

### 2.2. Preparation of films

Solution casting method was used to prepare CO incorporated gelatin-based films. Film-forming solutions (FFSs) of 10%, 15%, and 20% (w/w) gelatin was obtained separately after stirring gelatin solution on a magnetic stirrer 50 °C for 30 min at 1000 rpm. Constant glycerol (6%, w/w) amount was added to each FFS as a plasticizer. Initially, CO incorporated plasticized gelatin films were prepared by mixing CO with FFS to obtain 10% (w/w) virgin CO concentration at each gelatin concentration. Subsequently, CO was chemically homogenized by mixing with a surfactant, Tween 80, at 0.5%, 1%, 3% (v/w, based on FFS) concentration and mixed gradually with each FFS at 1000 rpm for 30 min. The most homogeneous films were determined. For further analysis, control film, GE film, was prepared from FFS of 20% (w/w) gelatin, 6%, (w/w) glycerol and 3% (v/w) Tween 80 without any CO content. GE-CO film was prepared by adding 10% (w/w) CO to FFS of GE film as mentioned above. FFS of 20 g was cast into Petri dishes with a diameter of 9.0 cm. The films were dried in a controlled environment at room temperature and a relative humidity (RH) of 40 ± 4%. Dried GE and GE-CO films had a thickness of 0.41 ± 0.15 mm and 0.35 ± 0.03 mm, respectively.

### 2.3. Characterization of physicochemical and thermal properties of films

#### 2.3.1. Moisture content, water uptake and water aging of the films

Moisture content, water uptake and water aging of GE films and GE-CO films were determined. Films were conditioned at 40%–50% RH for 72 h. Initial weight of samples were measured and moisture content of samples were calculated after films were dried at 30 °C until constant weight. Water uptake and water aging of the films were determined using a modified method (Parvez *et al* 2012). GE and GE-CO films were immersed in water at room temperature, collected and weighed after excess water was blotted out at different time intervals for determination of water absorption. All films, including replicates, were immersed in separate beakers and at each time interval, films were filtered through a filter paper to prevent mass loss until films were dissolved. Then films were dried in an environment at a temperature of 30 °C to a constant weight. Moisture content, water uptake and water aging (%) values were calculated in triplicates according to the equations (1)–(3), respectively where:  $W_i$  is the initial weight of the sample;  $W_f$ , is the final weight of the sample after soaking;  $W_d$ , is the dried weight of the sample:

$$\text{Moisture content (\%)} = \frac{W_i - W_d}{W_i} \times 100 \quad (1)$$

$$\text{Water uptake (\%)} = \frac{W_f - W_i}{W_i} \times 100 \quad (2)$$

$$\text{Water aging (\%)} = \frac{W_f - W_d}{W_f} \times 100. \quad (3)$$

#### 2.3.2. Scanning electron microscopy (SEM)

Microstructure of GE and GE-CO films containing 0% and 10% (w/w) CO, respectively, were analysed by a scanning electron microscope (Zeiss EVO® LS 10). Samples were completely dried and gold–palladium coated prior to examination. Images were obtained at an acceleration voltage of 5 kV.

#### 2.3.3. Fourier transform infrared spectroscopy (FTIR)

Samples of GE and GE-CO films containing 0% and 10% (w/w) CO, respectively, were analysed using Perkin Elmer Spectrum 400 FTIR spectrophotometer with attenuated total reflectance (ATR) technique. All the spectra were recorded in 650–4000  $\text{cm}^{-1}$  range, with a resolution of 2  $\text{cm}^{-1}$  after four scans.

#### 2.3.4. Differential scanning calorimetry (DSC)

Thermal analysis of GE and GE-CO films containing 0% and 10% (w/w) CO, respectively, were analysed by DSC using Perkin Elmer Pyris 1 DSC with heating at 10 °C  $\text{min}^{-1}$  from 10 °C to 445 °C. Three replicates of 6–10 mg were tested for each specimen.

### 2.4. Characterization of cell viability and *in vitro* wound healing

#### 2.4.1. L929 cell culture

L929 mouse skin fibroblasts, recommended by ISO standards for biological evaluation of biomaterials (Słota *et al* 2021), were used for XTT and Scratch Assays. Cells were cultured in DMEM-F12 premixed with 10% foetal bovine serum (FBS) and antibiotics (streptomycin 100  $\mu\text{g ml}^{-1}$  and penicillin 100 U  $\text{ml}^{-1}$ ) under 5%  $\text{CO}_2$  at 37 °C. After cells reached 80% of confluence, they were trypsinized, and counted using a hemocytometer (Marienfeld, Germany). Appropriate density of cells was seeded in T25 flasks and cultured until further usage of cells to conduct cell-based assays.

#### 2.4.2. XTT assay

In order to determine cell viability hence cytotoxicity, the effects of GE and GE-CO samples were analysed on mouse fibroblast cell line (L929) by carrying out XTT assay. Initially, L929 cells at a density of  $1 \times 10^4 \text{ well}^{-1}$  with DMEM-F12 were plated in a 96-well plate (TPP, Zurich, Switzerland) and cultured for overnight at 37 °C and 5%  $\text{CO}_2$  as mentioned above. After attachment of cells to the untreated bottom of cell culture plate, cells were washed with phosphate-buffered saline (PBS) twice. Prior to the assay, GE and GE-CO films in flasks were melted in water bath at 45 °C. Liquefied samples of GE and GE-CO films were brought to cell culture media temperature of 37 °C and then were added into DMEM-F12 medium containing phenol red to prevent pH change but no FBS to prevent cell proliferation at final concentrations of 5, 10, 15, 25, 50, 75 and 100  $\mu\text{g ml}^{-1}$  in triplicates and incubated for 24 h at 37 °C and 5%  $\text{CO}_2$  in a culture hood. Subsequently, XTT, 2,3-bis(2-metoksi-4-nitro-5-sulfofenil)-2H-tetrazolium, solution was added into wells and incubated at the same conditions for 4 h. Cell viability was measured at 570 nm wavelength by multiplate reader (Fluoroskan Ascent, Thermo Labsystems, Helsinki, Finland) and cytotoxicity was determined. In this assay control group for cell culture, i.e. 100% viable cells, was incubated with FBS but no CO.

#### 2.4.3. Scratch assay

Cells were seeded into 24 well plate at a density of  $6 \times 10^5 \text{ well}^{-1}$  with DMEM-F12 as mentioned above. Cells were incubated for 24 h at 37 °C and 5%  $\text{CO}_2$  for cell adhesion. To remove the FBS from cells, they were washed with PBS twice and then DMEM-F12 without FBS was added to cells again for starvation overnight. On the experiment day, GE and GE-CO films were turned into liquid form in flasks by melting them in water bath at 45 °C and liquefied GE and GE-CO samples were brought to cell culture medium temperature of 37 °C and then were added into DMEM-F12 medium containing phenol red to prevent pH change



but no FBS to prevent cell proliferation at final concentrations of 5, 10, 15, 25, 50, 75 and 100  $\mu\text{g ml}^{-1}$ . At the same time, a gap, i.e. a scratch was created in cell monolayer by direct manipulation for a physical cell exclusion (Chen 2012). After the scratch formation, wells were washed gently and cells were fed with GE and GE-CO containing media. Cells were incubated for 24 h at 37 °C and 5% CO<sub>2</sub>. Three replicates were used for each film at each concentration. In this assay, as negative control, L929 cell line incubated with DMEM-F12 basal medium containing neither CO nor FBS was used. As positive control, L929 cell line incubated with DMEM-F12 basal medium containing 5% FBS without any CO was used.

#### 2.4.4. Crystal violet staining

In order to detect adherent cells, crystal violet staining protocol by Feoktistova *et al* (2016) was carried out (Feoktistova *et al* 2016). Briefly, 3.7% paraformaldehyde, 1% crystal violet dye and glycerol in 2% ethanol were prepared as experimental solutions. The medium on the cells was removed and then cells were washed with PBS. Paraformaldehyde was added to the cells and incubated at room temperature for 30 min. After that, paraformaldehyde on the cells was removed and stained with crystal violet for 30 min at room temperature. Then the dye on the cells was removed and the cells were washed two times with tap water. Excess water on the cells was removed and stained cells were examined after adding glycerol via microscope.

#### 2.4.5. Statistical analysis

Statistical analysis to determine any significant difference between GE and GE-CO films' influence on cell viability at 5, 10, 15, 25, 50, 75 and 100  $\mu\text{g ml}^{-1}$  concentration; and to determine any significant difference of cell viability between 100% viable control group and each film at each concentration were carried out using one way analysis of variance followed by Tukey's HSD (honestly significant difference) test. IBM SPSS Statistics 24 version was used for analyses. Experiments were carried out in triplicates with significance threshold set at  $P$  value < 0.05.

## 3. Results and discussion

### 3.1. Homogenous film production

Films containing 10% and 15% (w/w) gelatin were brittle and difficult to peel from the Petri dish, therefore, gelatin concentration was increased to 20% (w/w) and FFS of gelatin films were plasticized with glycerol which further improved handling of gelatin films (Vanin *et al* 2005). Biopolymer based films have a brittle nature and since ideal wound dressing materials are flexible and stretchable, plasticizer incorporation is necessary for gelatin based wound dressing materials (Sezer and Cevher 2011, Zaman *et al* 2011,

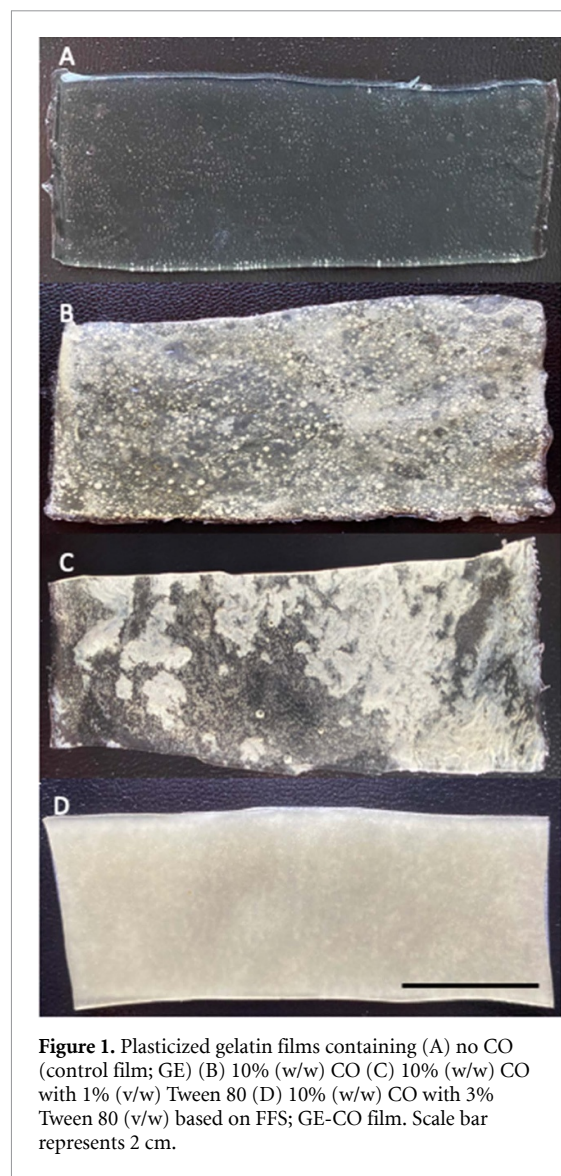
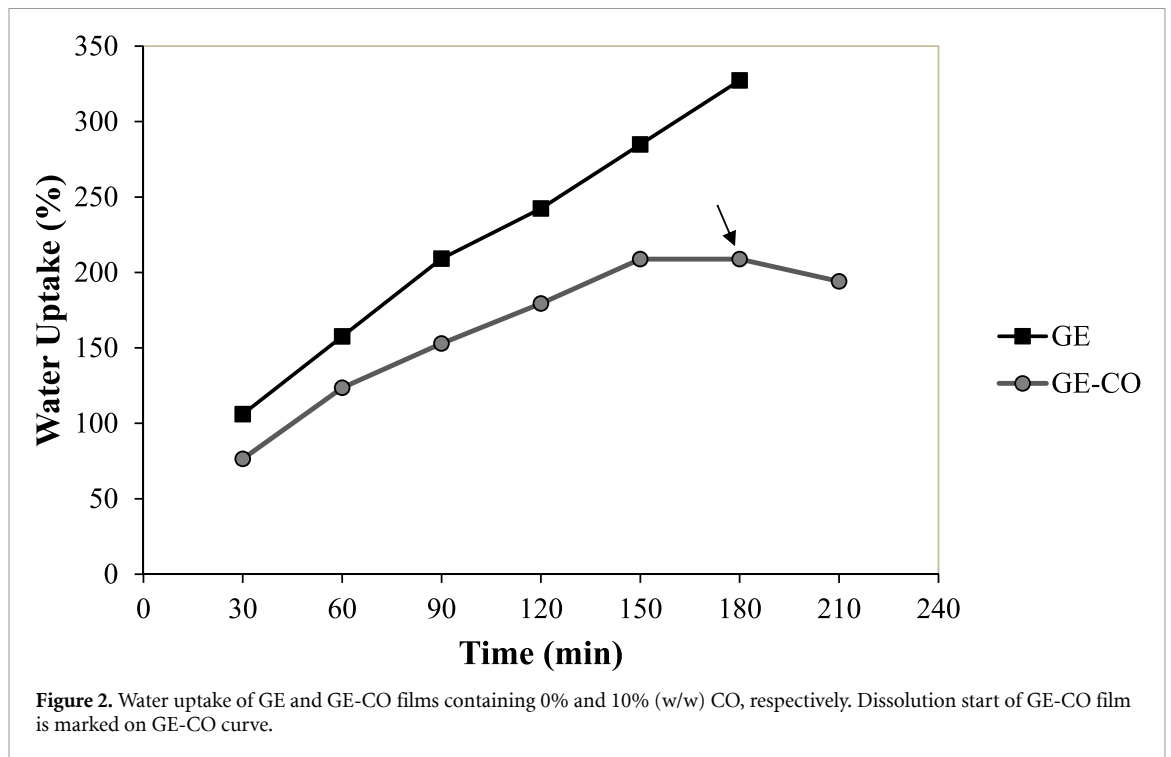


**Figure 1.** Plasticized gelatin films containing (A) no CO (control film; GE) (B) 10% (w/w) CO (C) 10% (w/w) CO with 1% (v/w) Tween 80 (D) 10% (w/w) CO with 3% Tween 80 (v/w) based on FFS; GE-CO film. Scale bar represents 2 cm.

Conzatti *et al* 2018). All plasticized control films containing 20% (w/w) gelatin were transparent and morphologically similar whether they contained Tween 80 or not (figure 1(A)). Partly opaque and heterogeneous films were obtained when 10% (w/w) CO was added to the FFS (figure 1(B)). Surfactant incorporation is required in formation of emulsion films for uniform oil droplet distribution (Tongnuanchan *et al* 2014). A non-ionic surfactant with minimal toxicity, Tween 80, was added to protein based films previously for mainly food packaging applications (Varma *et al* 1985, Bahram *et al* 2014, Tongnuanchan *et al* 2014). Therefore, to obtain more homogenous films in the presence of CO, some Tween 80 concentrations (0.5%–3%, v/w, based on FFS) were mixed with CO and added to FFS. When films contained Tween 80 at 0.5% and 1% (v/w), films were still heterogeneous (figure 1(C)). Homogeneity of films were improved when Tween 80 concentration was increased to 3% (v/w) since a more uniform distribution of CO in protein network of 20% (w/w) gelatin films was



obtained. Therefore, further analyses were conducted on GE-CO films that contained 20% (w/w) plasticized gelatin and 10% (w/w) CO mixed with 3% (v/w) Tween 80 in the FFS and compared with control films, GE, with the same composition without any CO content.

### 3.2. Effect of CO on physicochemical and thermal properties of films

#### 3.2.1. Moisture content, water uptake, water aging of the films

Moisture content, water uptake and water aging of GE-CO film were determined and compared with GE film. Hydrophobicity of CO decreased moisture content of the film since moisture content of GE-CO was  $41.0 \pm 0.13\%$  and GE was  $47.5 \pm 2.5\%$ .

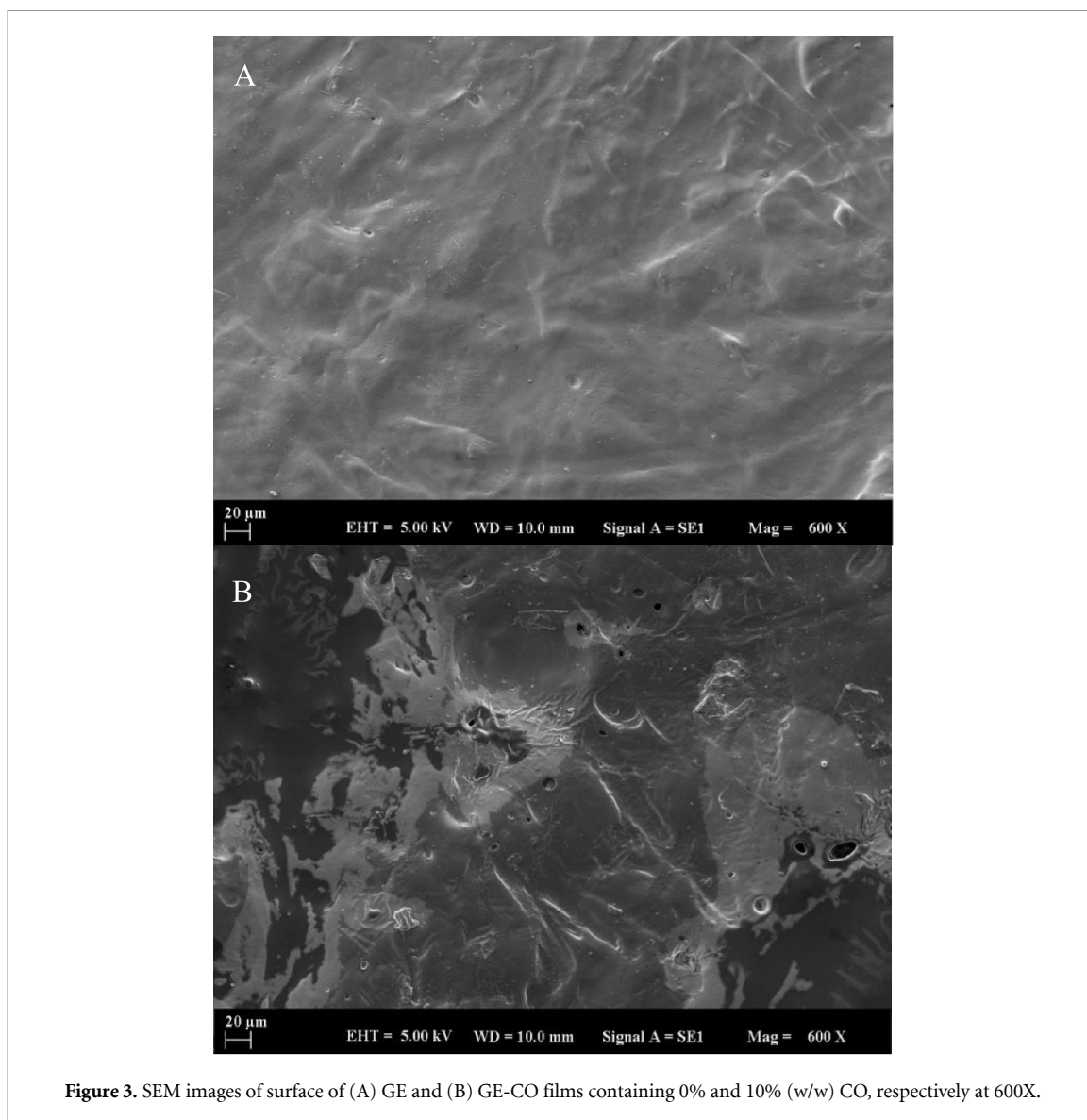
Water uptake of GE and GE-CO films are shown in figure 2. Water uptake is an essential feature of wound dressing materials to absorb exudes from the wound site (Mao *et al* 2003, Parvez *et al* 2012). Gelatin is a hydrophilic polymer, therefore its water uptake was rapid and increased with time in both samples, however, after 3 h in water, GE film had more water uptake percentage, 327%, than GE-CO film, 208%, due to the hydrophobic nature of oil. Although incorporation of CO decreased water uptake of the films when compared with GE film, water uptake percentage was still high (>200%) to absorb the exudes from the wound.

Moreover, CO content in the film increased durability of the biomaterial in water since GE-CO film became saturated after 2.5 h and started to dissolve after 3 h decreasing the weight of the film which led

to less water uptake. Subsequently, GE-CO film dissolved completely after 3.5 h in water. However, GE film dissolved rapidly after 3 h in water and since the net weight of the film decreased significantly due to dissolution, the remaining films' water uptake data is not shown. In other studies, when pure gelatin film was studied as a wound dressing material, it dissolved after less than 10 min in water (Zaman *et al* 2011, Parvez *et al* 2012). Incorporation of chitosan to gelatin retained wound dressing material for 40 min in water (Parvez *et al* 2012). Therefore, in this study, incorporation of CO content along with glycerol and Tween 80 has improved gelatin films as wound dressing materials. In relation to this, water aging of GE film was  $87.5 \pm 0.9\%$ , while GE-CO film had lower water aging percentage of  $81.9 \pm 0.3\%$ , which is a preferred characteristic of a wound dressing material (Parvez *et al* 2012).

#### 3.2.2. Structure of films

SEM was used to analyse microstructure of GE and GE-CO films. Despite the presence of some holes about  $\sim 2 \mu\text{m}$  diameter, the surface of GE film was more continuous without the formation of a separate phase and smoother than the oil incorporated film (figure 3(A)). Due to immiscibility of oil with water, phase separation in film matrix was observed on the surface of GE-CO film despite the addition of the surfactant (figure 3(B)). Similarly, in another study it was suggested that oil was separated from aqueous phase due to hydrophobic nature of oil (Atarés *et al* 2010). Moreover, formation of bigger pores,  $\sim 5\text{--}25 \mu\text{m}$ , caused the surface of GEL-CO film to be rougher



than GE film. Similarly in other studies, incorporation of oils to protein based films caused discontinuity throughout the film matrix with a rougher surface due to the presence of two immiscible phases when observed via SEM (Fernández-Pan *et al* 2012, Yeddes *et al* 2020). In the aforementioned studies, hydrophobicity of oil disrupted uniformity of films in spite of homogenization of oil and therefore, oil droplets were observed in protein matrix (Fernández-Pan *et al* 2012, Yeddes *et al* 2020, Kilinc *et al* 2021). Similarly in another study, phase separation was observed via SEM when several different oils were incorporated to gelatin based films despite the chemical homogenization by different surfactants including Tween 80 and also the mechanical homogenization (Tongnuanchan *et al* 2014). Tongnuanchan *et al* (2014) suggested that concentration of oil phase towards film surface, i.e. creaming, and phase separation during drying of films after casting would occur in films containing oil despite the addition of surfactants (Tongnuanchan *et al* 2014).

The molecular structure of GE and GE-CO films with 0% and 10% (w/w) CO were investigated by ATR-FTIR analysis (figures 4(A) and (B)), respectively. Gelatin is a protein and its main units, amino acids, are joined by amide bonds. Therefore, characteristic infrared (IR) absorption bands such as amide-A and I–III are mainly determined from polypeptide and protein repeat units and identified in both samples (Kong and Yu 2007, Das *et al* 2017). The main information of gelatin structure is generally determined from the region of  $3000\text{--}3600\text{ cm}^{-1}$  and  $1100\text{--}1700\text{ cm}^{-1}$  on the FTIR spectrum (Neumann *et al* 1981, Pawde and Deshmukh 2008). Amide-A band showing NH-stretching involved in hydrogen bonding corresponds to wavelength at  $\sim 3300\text{ cm}^{-1}$  (Tongnuanchan *et al* 2014). Amide-A peak of GE had higher amplitude corresponding to higher free-amino groups than GE-CO (Chuaynukul *et al* 2018). In accordance with this, amide-A peak was situated at  $3318\text{ cm}^{-1}$  in GE but shifted to a lower frequency of  $3292\text{ cm}^{-1}$  in GE-CO film indicating more NH

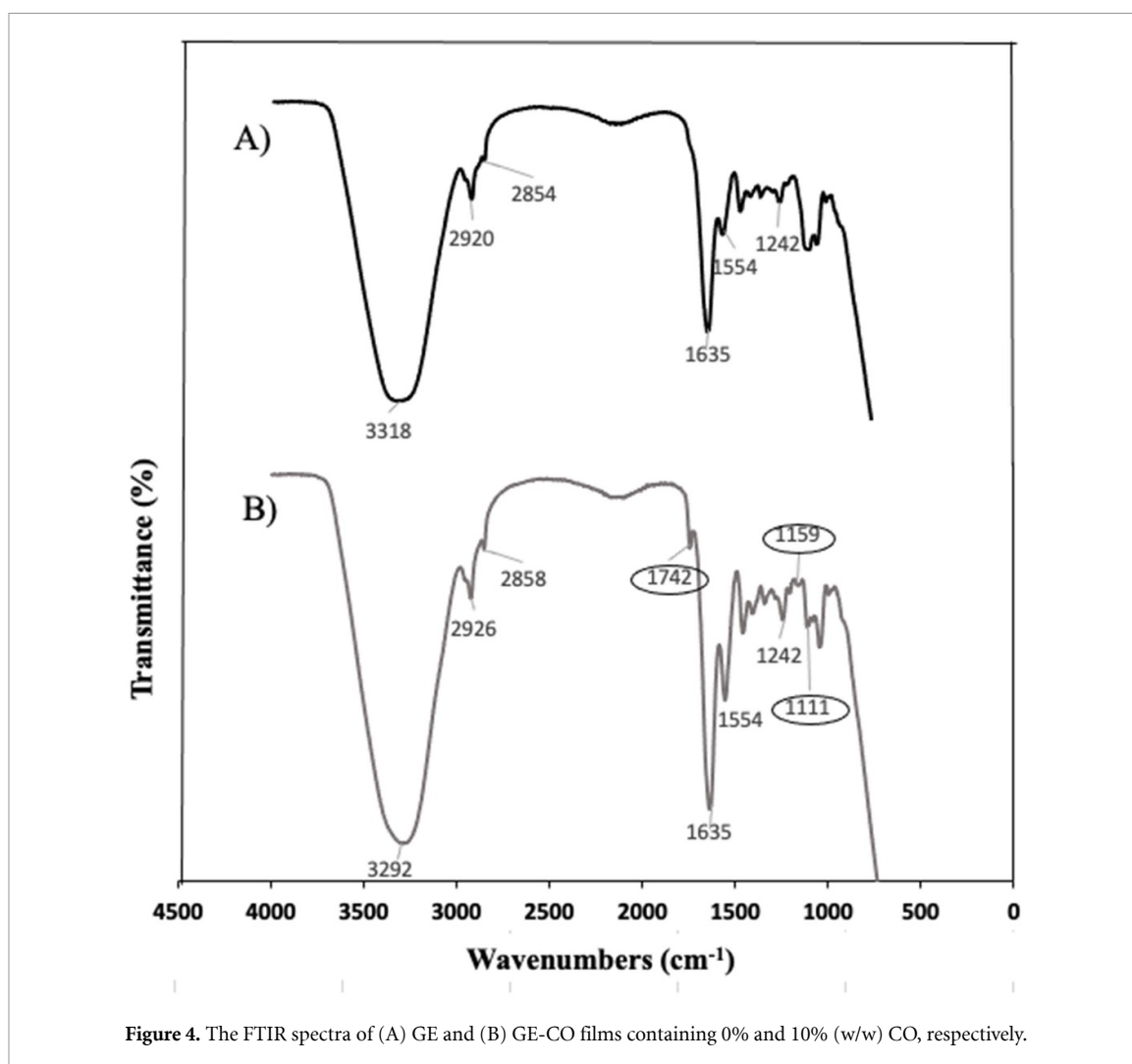


Figure 4. The FTIR spectra of (A) GE and (B) GE-CO films containing 0% and 10% (w/w) CO, respectively.

groups of gelatin was involved in hydrogen bonding when films contained CO (Chuaynukul *et al* 2018). Peak at  $1635\text{ cm}^{-1}$  in both samples was attributed to occurrence of amide-I band of gelatin showing C=O stretching (Das *et al* 2017). Amide-II and amide-III peaks were placed at  $1554$  and at  $1242\text{ cm}^{-1}$ , respectively in both films (Das *et al* 2017). These peaks also correspond to presence of free water (Bergo and Sobral 2007). The peaks situated around  $2924$  and  $2854\text{ cm}^{-1}$  were assigned to be asymmetric and symmetric stretching vibrations of the methylene functional group, respectively; and identified in films containing gelatin and glycerol previously (Guillén and Cabo 2004, Tongnuanchan *et al* 2014). These peaks were situated at  $2920$  and  $2854\text{ cm}^{-1}$  in GE and they shifted to higher wavelengths of  $2926$  and  $2858\text{ cm}^{-1}$  in GE-CO with similar amplitudes. Wavelength and amplitude differences are reported to be related to the interaction between functional groups of protein and the oil content (Bahram *et al* 2014, Tongnuanchan *et al* 2014).

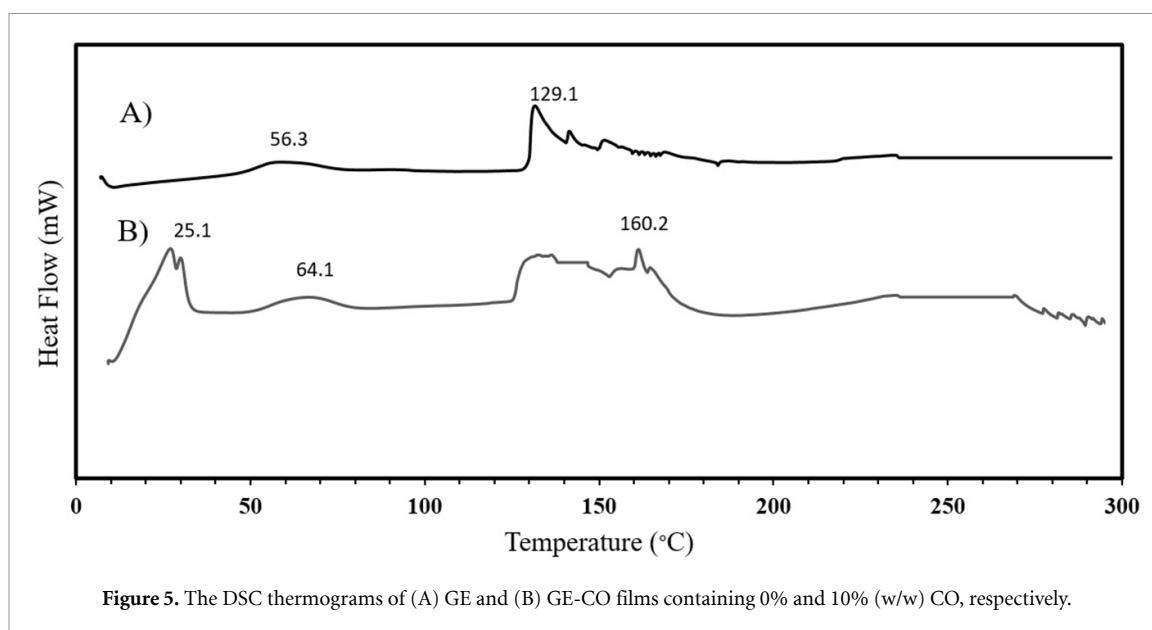
Triglyceride component of CO was observed only in FTIR spectra of GE-CO film (figure 4(B)) (Rohman *et al* 2010). C=O stretching vibration of

aldehyde or carbonyl ester group, chemical group of oils, was observed at the peak observed at  $1742\text{ cm}^{-1}$  (Mohamed *et al* 2010, Rohman *et al* 2010, Tongnuanchan *et al* 2014). -C-O stretching peaks at wavelength of  $1159$  and  $1111\text{ cm}^{-1}$  were characterized from virgin CO previously (Rohman *et al* 2010) and were only observed when samples contained CO in this study.

### 3.2.3. Thermal analysis of films

DSC was used to characterize influence of CO on thermal transitions of gelatin films. Thermal transitions such as glass transition ( $T_g$ ) is related to the mobility of amorphous, i.e. less ordered, structure of gelatin; and melt-like transition ( $T_{max}$ ) is related to the temperature that disrupts the ordered structure of proteins (Chuaynukul *et al* 2018). GE showed  $T_g$  at  $56.3\text{ }^\circ\text{C}$  which was followed by endothermic peaks, at a maximum temperature of ( $T_{max}$ )  $129.1\text{ }^\circ\text{C}$  (figure 5). Similarly in another study, mostly anhydrous bovine gelatin-cast films exhibited  $T_g$  at  $53\text{ }^\circ\text{C}$  which was followed by an endothermic peak (Chuaynukul *et al* 2018). In another study,  $T_{max}$  of gelatin films were  $\sim 148\text{ }^\circ\text{C}$  (Sobral *et al* 2001).



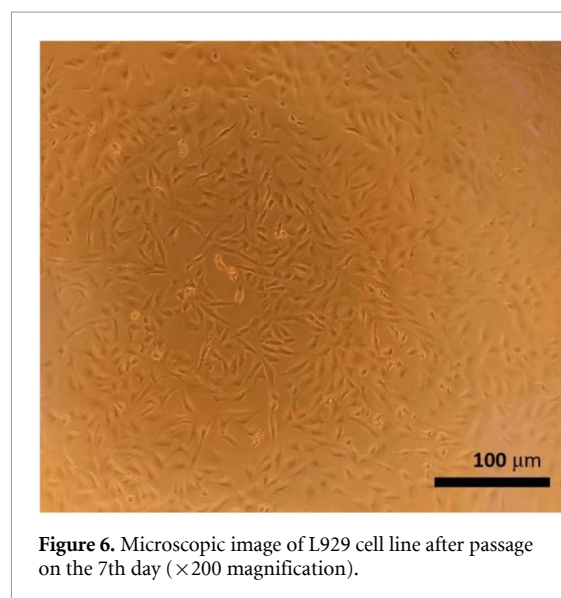


In GE-CO films, an endothermic peak was only observed at 25.1 °C which corresponds to melting temperature of CO (Srivastava *et al* 2017). Also,  $T_g$  of GE-CO increased to 64.1 °C. Previously, it was determined that increase in amount of water yields amorphous phase that decreases  $T_g$  of gelatin films (Sobral *et al* 2001). Moisture content of GE-CO film was lower than GE, which led to an increase in  $T_g$  of GE-CO. Endothermic peaks were observed after  $T_g$  and the maximum peak was at 160.2 °C which was higher than  $T_{max}$  of GE film. The increase in  $T_{max}$  suggested higher molecular order of gelatin film when contained CO (Tongnuanchan *et al* 2014). Instead of a single peak, many endothermic peaks were observed after  $T_g$  in both films. However, broader endothermic peaks appeared in GE-CO films indicating thermal improvement of the films which is similar to another study when polysaccharide films contained CO, instead of a single peak, broader endothermic peaks were observed near melting point of the films (Ismail *et al* 2014). Moreover, greater melting enthalpy, ( $\Delta H$ ) 75.2 J g<sup>-1</sup>, was required for disruption of interchain reaction for GE-CO film, whereas  $\Delta H$  of GE film was 64.4 J g<sup>-1</sup> (Tongnuanchan *et al* 2014). Therefore, more energy is necessary to disrupt gelatin film when CO is incorporated due to the higher molecular order of the film.

### 3.3. Effect of CO on cell viability and wound healing

#### 3.3.1. L929 cell culture

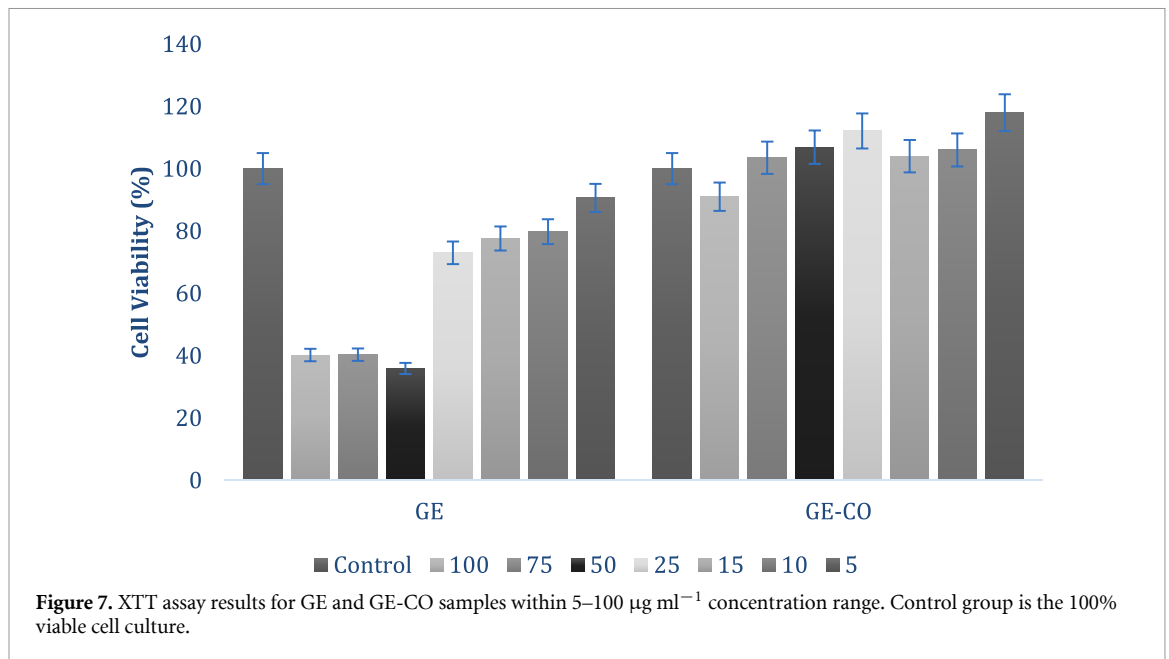
L929 mouse skin fibroblast cell line was used for both XTT and Scratch Assays to evaluate the influence of CO on cell viability and wound healing, respectively, since it is recommended by ISO standards for biological evaluation of biomaterials which are intended to be used for biotechnological and medical applications (Słota *et al* 2021). L929 mouse



fibroblast cell line was used in other studies for cytotoxicity and/or scratch assays as well (Yousefi *et al* 2017, Çınar 2020, Słota *et al* 2021). Fibroblasts are normally abundant in connective tissues and responsible for tissue homeostasis, however, when tissues are injured fibroblasts become activated to aid in reconstituting the integrity of the skin (Li and Wang 2011, Qadir *et al* 2021). Fibroblast cells are essential for wound healing and fibroblast growth factor (FGF) is one of the cytokines that are effective in early periods of the healing process (Öztopalan *et al* 2017, Baktir 2019). Therefore, fibroblast cell line is one of the cell lines suggested in literature to study *in vitro* wound healing (Baktir 2019).

L929 cells were incubated in culture hood and were observed by an inverted microscope daily. Cells appeared to have healthy and intact characteristics (figure 6). These non-treated cells were prepared to be used in cellular assays.





### 3.3.2. XTT assay

XTT assay as a measure of cell viability was carried out to obtain the non-toxic and potential proliferative concentrations of liquefied GE and GE-CO samples within the concentration range of 5–100  $\mu\text{g ml}^{-1}$ . In the assay, the effect of CO on inhibition of cell growth was assessed as cell viability percentage. Non-treated cells were taken as 100% viable which is the control group of cell culture that was incubated with FBS without CO. Cell viability results showed that GE films significantly decreased cell viability at 10–100  $\mu\text{g ml}^{-1}$  concentrations when compared with 100% viable cell culture control group ( $P < 0.05$ ) (figure 7). Moreover, GE films were toxic for L929 at concentrations of 100, 75 and 50  $\mu\text{g ml}^{-1}$  since these samples without CO decreased  $\sim 50\%$  of the viability. When compared with GE-CO, viability of GE treated cells were significantly lower than viability of cells treated with GE-CO samples at any concentration ( $P < 0.05$ ). Therefore, CO increased cell viability significantly when compared to film samples without CO ( $P < 0.05$ ).

Replicate assays present that the CO incorporated biomaterial has a potential proliferative effect on L929 cells at any concentration within 5–100  $\mu\text{g ml}^{-1}$  range which correspond to cell viability of  $\sim 100\%$  (figure 7). Cell viability was not significantly different than the 100% viable control group when cells were incubated with GE-CO at 100, 75, 50  $\mu\text{g ml}^{-1}$  concentrations ( $P > 0.05$ ), however, viability was significantly higher than the 100% viable control group when GE-CO was within 5–25  $\mu\text{g ml}^{-1}$  concentration range ( $P < 0.05$ ) which shows a potential proliferative effect of GE-CO film samples as increase in daughter cell population indicate cell proliferation (Gratzner 1982, Khan 2019). This modest

and acceptable increase in the viability of L929 cells demonstrates that GE-CO is non-toxic to L929 at the given concentration range and is a promising biomaterial as a wound dressing material.

There are restricted studies about cytotoxicity of CO on fibroblast cell lines in literature. However, a study also showed that virgin CO is non-cytotoxic for human fibroblast cells until 72 h of culture which is consistent with our data (Ismail *et al* 2014). In another study, when oral fibroblast cells were treated with 1-monolaurin, a natural compound of CO, doses up to 2500  $\mu\text{M}$  were reported to be non-toxic for the oral fibroblasts (Seleem *et al* 2016).

### 3.3.3. Scratch assay

Wound healing is a process that comprises four phases which may also overlap: Hemostasis, inflammation, proliferation and maturation (Guo and DiPietro 2010, Park *et al* 2011). The important phase of this process that will trigger cell proliferation and wound closure is the inflammatory phase in which several cytokines such as FGF are seen effectively (Guo and DiPietro 2010, Öztöpalan *et al* 2017). Then, during proliferation phase which may overlap with inflammatory phase fibroblast cells migrate to wound site to form granulation tissues (Malinda *et al* 1998, Werner *et al* 2007, Guo and DiPietro 2010, Alven *et al* 2021). Due to FGF in the wound site, keratinocytes proliferate and the final phase of wound healing proceeds (Werner *et al* 2007). Some of the existing fibroblasts transform into myofibroblasts, which have a role in contraction of wound site, to facilitate wound closure (Li and Wang 2011). Under normal circumstances, fibroblasts are abundant in connective tissues and responsible for tissue homeostasis, however, when tissues are injured fibroblasts become activated (Li and

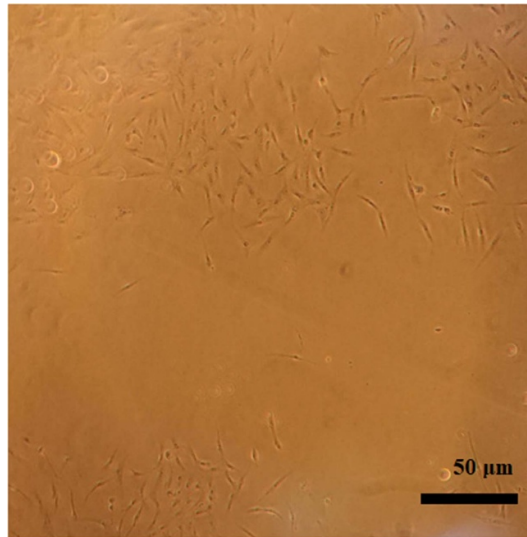


**Figure 8.** Microscopic observation of cell deterioration when L929 cells were incubated with GE samples ( $t = 24$  h,  $200\times$ ).

Wang 2011). Therefore, it is necessary to see the presence, the increase and the continuity of fibroblasts in wound site for healing (Baktir 2019).

For this purpose, in this study, confluent L929 cells culture was used for scratch assay. Fibroblast cell line was also used in other studies for scratch assay as well (Walter *et al* 2010, Yousefi *et al* 2017). Migration of cells and fast wound closure were observed in L929 fibroblast scratch assay when healing was monitored for 24 h using inverted microscopy (Walter *et al* 2010). In another study when L929 mouse skin fibroblasts were used to determine the effect of Gossypin on wound healing, effective migration of fibroblasts were observed (Çinar 2020). In our study, liquefied samples of GE and GE-CO films were mixed with the cell culture medium at  $5\text{--}100\ \mu\text{g ml}^{-1}$  concentrations and added to the cell culture dishes containing cells to examine the effects of GE and GE-CO samples on cell migration.

When observed via microscopy, previously adherent L929 cells detached from the bottom of microplate wells upon incubation with GE samples (figure 8). Cells lose their adherence when they undergo cell death (Feoktistova *et al* 2016). Therefore, GE samples at any concentration within  $5\text{--}100\ \mu\text{g ml}^{-1}$  range, caused detachment of cells as a result of deterioration of cells. Similarly, in another study, gelatin promoted L929 cell detachment (Wang *et al* 2016). This result in accordance with XTT assay result since GE samples decreased cell viability significantly ( $P < 0.05$ ), and were toxic for L929 at 100, 75 and  $50\ \mu\text{g ml}^{-1}$  concentrations which decreased  $\sim 50\%$  of the viability of cells. Thus, healing potential could not be determined by scratch assay when gelatin-based films did not contain CO. Therefore, the progression of healing is observed by comparing

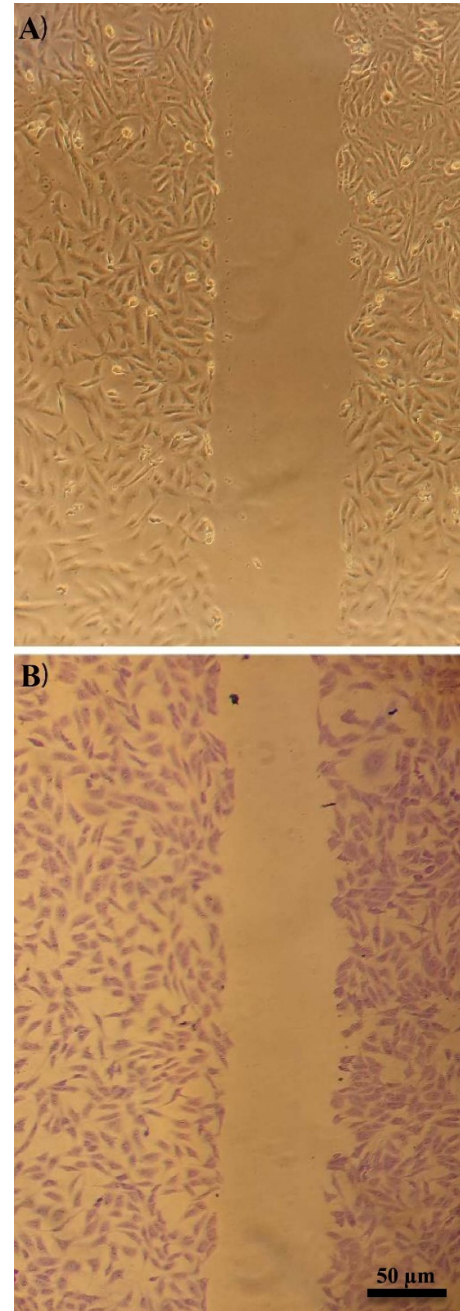


**Figure 9.** Microscopic images of scratch formation on L929 at  $t = 0$  h,  $200\times$  (A) negative control group, to be incubated with basal medium containing neither CO nor FBS, (B) to be incubated with GE-CO biomaterial samples at  $5$  or  $10\ \mu\text{g ml}^{-1}$  concentration.

the effect of GE-CO with a negative control group of cell culture after scratch formation (figure 9(A)), in which cells were incubated with basal medium that contained neither CO nor FBS. Figure 9(B) shows scratch formation on cells before incubation with GE-CO samples. In negative control group of cell culture, no closure of scratch was observed after 24 h and due to the change in morphology of the cells, gap of the scratch was enlarged (figure 10(A)). However, when cells were incubated with GE-CO samples, cells survived and the highest closure of the scratch was observed after 24 h when GE-CO samples were at 5



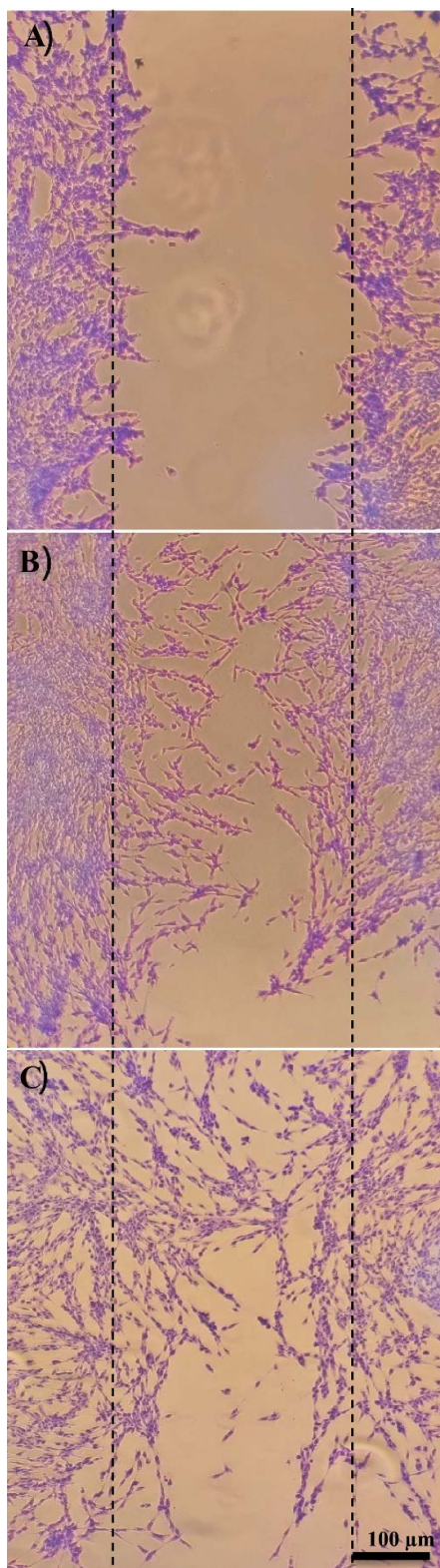


**Figure 10.** Microscopic images of L929, at  $t = 24$ th hour,  $100\times$  (A) negative control group that was incubated with basal medium containing neither CO nor FBS, (B) incubated with GE-CO biomaterial samples at  $5\ \mu\text{g ml}^{-1}$  and (C) at  $10\ \mu\text{g ml}^{-1}$  concentration.

and  $10\ \mu\text{g ml}^{-1}$  concentrations (figures 10(B) and (C), respectively) similar to FBS containing positive control group of cell culture (data not shown) which

indicates healing. It is observed that cell morphologies had a spindle shape and a directional orientation towards the injured area. In another study, normal human skin fibroblast cells were also reported to be in elongated/spindle shape after a 72 h long incubation with gellan gum based biomaterials some containing CO which shows that a morphological change in cells can be encountered during incubation (Ismail *et al* 2014). The result of the scratch assay is in accordance with XTT results where cell viability was  $\geq 100\%$  when cells were treated with GE-CO films which is an indication of an increase in daughter cell population, i.e. cell proliferation.

#### 4. Conclusion

In this study, the influence of CO on gelatin-based film properties and *in vitro* healing were determined for wound dressing applications. Homogenous and continuous GE-CO film was obtained for 10% (w/w) CO with 3% (v/w) Tween 80 in the FFS of 20% (w/w) plasticized gelatin. Although hydrophobic, CO content did not prevent water uptake of the films since water uptake is an essential property of wound dressing materials (Parvez *et al* 2012). Microstructure of films showed that CO incorporation caused a rougher surface of gelatin-based films due to hydrophobic nature of oil. Structural changes due to triglyceride component and increased hydrogen bonding between NH groups of gelatin were observed in GE-CO samples by FTIR analysis. Thermal properties of the films were improved due to the CO content since melt-like transition temperature and melting enthalpy of GE-CO film were higher than GE film. Effect of CO on cell viability and cell migration were determined on L929 cell line. Obtained cell culture results showed that CO content of GE-CO samples caused a significant increase in cell viability at any concentration within  $5\text{--}100\ \mu\text{g ml}^{-1}$  range when compared with GE films ( $P < 0.05$ ). Moreover, when compared with 100% viable control group of cell culture, GE samples within  $10\text{--}100\ \mu\text{g ml}^{-1}$  concentration range decreased cell viability significantly ( $P < 0.05$ ), and were toxic for L929 at concentrations of  $100$ ,  $75$  and  $50\ \mu\text{g ml}^{-1}$  which decreased  $\sim 50\%$  of the viability. However, GE-CO samples maintained cell viability similar to 100% viable control group and had a potential proliferative effect when cell culture was incubated with GE-CO samples within  $5\text{--}25\ \mu\text{g ml}^{-1}$  concentration range. Scratch Assay showed that GE-CO samples accelerated migration of cells and closure of scratch as an indication of healing. However, when cell culture was incubated with GE samples, L929 cells detached from the bottom of microplate wells as a result of deterioration of cells. Therefore, CO content in the films not only maintained cell viability but also enabled cells to migrate and proliferate efficiently. Results reported in this study showed that CO could be incorporated to

gelatin-based films for preparation of a wound dressing biomaterial which is also demonstrated to have a promising *in vitro* wound healing effect.

### Data availability statement

All data that support the findings of this study are included within the article (and any supplementary files).

### Acknowledgment


The authors would like to thank Assoc. Professor Rabia Cakir-Koc for sharing the infrastructure for cell culture with us.

### Funding

This study has been funded by Istanbul Gelişim University Scientific Research Projects Application and Research Center (Project No. DUP-220220-MK).

### ORCID iDs

Mehlika Karamanlioglu  <https://orcid.org/0000-0002-4814-6346>

Serap Yesilkir-Baydar  <https://orcid.org/0000-0001-6311-4302>

### References

- Akhavan-Kharazian N and Izadi-Vasafi H 2019 Preparation and characterization of chitosan/gelatin/nanocrystalline cellulose/calcium peroxide films for potential wound dressing applications *Int. J. Biol. Macromol.* **133** 881–91
- Alkekhia D, Hammond P T and Shukla A 2020 Layer-by-layer biomaterials for drug delivery *Annu. Rev. Biomed. Eng.* **22** 1–24
- Alven S, Khwaza V, Oyedeji O O and Aderibigbe B A 2021 Polymer-based scaffolds loaded with aloe vera extract for the treatment of wounds *Pharmaceutics* **13** 7
- Ambika A P and Nair S N 2019 Wound healing activity of plants from the convolvulaceae family *Adv. Wound Care* **8** 28–37
- Atarés L, Bonilla J and Chiralt A 2010 Characterization of sodium caseinate-based edible films incorporated with cinnamon or ginger essential oils *J. Food Eng.* **100** 678–87
- Bahram S, Rezaei M, Soltani M, Kamali A, Ojagh S M and Abdollahi M 2014 Whey protein concentrate edible film activated with cinnamon essential oil *J. Food Process. Preserv.* **38** 1251–8
- Baktir G 2019 Wound repair and experimental wound models *Experimed* **9** 130–7
- Bergo P and Sobral P J A 2007 Effects of plasticizer on physical properties of pigskin gelatin films *Food Hydrocoll.* **21** 1285–9
- Chen Y 2012 Scratch wound healing assay *Bio-Protocol* **2** e100
- Cheng L *et al* 2020 Injectable polypeptide-protein hydrogels for promoting infected wound healing *Adv. Funct. Mater.* **30** 2001196
- Chuaynukul K, Nagarajan M, Prodpran T, Benjakul S, Songtipya P and Songtipya L 2018 Comparative characterization of bovine and fish gelatin films fabricated by compression molding and solution casting methods *J. Polym. Environ.* **26** 1239–52
- Çınar İ 2020 Gossypin'in L929 Fibroblast Hücrelerindeki Hidrojen Peroksit Hasarına Karşı Koruyucu Etkilerinin Değerlendirilmesi *Kafkas J. Med. Sci.* **10** 15–23
- Conzatti G, Chamary S, de Geyter N, Cavalie S, Morent R and Tourrette A 2018 Surface functionalization of plasticized chitosan films through PNIPAM grafting via UV and plasma graft polymerization *Eur. Polym. J.* **105** 434–41
- Das M P, PR S, KA P, Jv V and Renuka M 2017 Extraction and characterization of gelatin: a functional biopolymer *Int. J. Pharm. Pharm. Sci* **9** 239
- Dayrit F M 2015 The properties of lauric acid and their significance in coconut oil *J. Am. Oil Chem. Soc.* **92** 1–15
- Feoktistova M, Geserick P and Leverkus M 2016 Crystal violet assay for determining viability of cultured cells *Cold Spring Harb. Protoc.* **2016** pdb-prot087379
- Fernández-Pan I, Royo M and Ignacio Mate J 2012 Antimicrobial activity of whey protein isolate edible films with essential oils against food spoilers and foodborne pathogens *J. Food Sci.* **77** M383–90
- Gratzner H G 1982 Monoclonal antibody to 5-bromo- and 5-iododeoxyuridine: a new reagent for detection of DNA replication *Science* **218** 474–5
- Grzybowski J, Kolodziej W, Trafny E A and Struzyna J 1997 A new anti-infective collagen dressing containing antibiotics *J. Biomed. Mater. Res.* **36** 163–6
- Guillén M D and Cabo N 2004 Study of the effects of smoke flavourings on the oxidative stability of the lipids of pork adipose tissue by means of Fourier transform infrared spectroscopy *Meat Sci.* **66** 647–57
- Guo S A and DiPietro L A 2010 Factors affecting wound healing *J. Dent. Res.* **89** 219–29
- Hajjalyani M, Tewari D, Sobarzo-Sánchez E, Nabavi S M, Farzaei M H and Abdollahi M 2018 Natural product-based nanomedicines for wound healing purposes: therapeutic targets and drug delivery systems *Int. J. Nanomed.* **13** 5023–43
- Huang Y, Zhao X, Zhang Z, Liang Y, Yin Z, Chen B, Bai L, Han Y and Guo B 2020 Degradable gelatin-based IPN cryogel hemostat for rapidly stopping deep noncompressible hemorrhage and simultaneously improving wound healing *Chem. Mater.* **32** 6595–610
- Huang Z, Tian Z, Zhu M, Wu C and Zhu Y 2021 Recent advances in biomaterial scaffolds for integrative tumor therapy and bone regeneration *Adv. Ther.* **4** 2000212
- Indurkar A, Pandit A, Jain R and Dandekar P 2021 Plant-based biomaterials in tissue engineering *Bioprinting* **21** e00127
- Ismail N A, Amin K A M and Razali M H 2018 Mechanical and antibacterial activities study of gellan gum/virgin coconut oil film embedded norfloxacin *IOP Conf. Ser.: Mater. Sci. Eng.* **440** 012001
- Ismail N A, Mohamad S F, Ibrahim M A and Mat Amin K A 2014 Evaluation of gellan gum film containing virgin coconut oil for transparent dressing materials *Adv. Biomater.* **2014** 1–12
- Khan Y 2019 Characterizing the properties of tissue constructs for regenerative engineering *Encyclopedia of Biomedical Engineering* ed B E Narayan (Amsterdam: Elsevier) pp 537–45
- Kilinc D, Ocak B and Özdestan-Ocak Ö 2021 Preparation, characterization and antioxidant properties of gelatin films incorporated with *Origanum onites* L. essential oil *J. Food Meas. Character.* **15** 795–806
- Kim H S, Kumbar S G and Nukavarapu S P 2021 Biomaterial-directed cell behavior for tissue engineering *Curr. Opin. Biomed. Eng.* **17** 100260
- Kong J and Yu S 2007 Fourier transform infrared spectroscopic analysis of protein secondary structures *Acta Biochim. Biophys. Sin.* **39** 549–59
- Li B and Wang J H-C 2011 Fibroblasts and myofibroblasts in wound healing: force generation and measurement *J. Tissue Viability* **20** 108–20
- Makvandi P, Ali G W, Della Sala F, Abdel-Fattah W I and Borzacchiello A 2020 Hyaluronic acid/corn silk extract based injectable nanocomposite: a biomimetic antibacterial scaffold for bone tissue regeneration *Mater. Sci. Eng. C* **107** 110195



- Malinda K M, Sidhu G S, Banaudha K K, Gaddipati J P, Maheshwari R K, Goldstein A L and Kleinman H K 1998 Thymosin  $\alpha$ 1 stimulates endothelial cell migration, angiogenesis, and wound healing *J. Immunol.* **160** 1001–6
- Mao J, Zhao L, de Yao K, Shang Q, Yang G and Cao Y 2003 Study of novel chitosan-gelatin artificial skin *in vitro* *J. Biomed. Mater. Res. A* **64** 301–8
- Matsuda K, Suzuki S, Isshiki N and Ikada Y 1993 Re-freeze dried bilayer artificial skin *Biomaterials* **14** 1030–5
- Muktar M Z, Rose L B C and Amin K A M 2017 Formulation and optimization of virgin coconut oil with Tween-80 incorporated in gellan gum hydrogel *AIP Conf. Proc.* **1885** 020044
- Mohamed A A, El-Emary G A and Ali H F 2010 Influence of some citrus essential oils on cell viability, glutathione-S-transferase and lipid peroxidation in Ehrlich ascites carcinoma cells *J. Am. Sci.* **6** 820–6 (available at: [www.americanscience.org](http://www.americanscience.org)) (Accessed 6 June 2021)
- Montero P, Gómez-Guillén M C and Borderias A J 1999 Functional characterisation of muscle and skin collagenous material from hake (*Merluccius merluccius* L.) *Food Chem.* **65** 55–59
- Muktar M Z, Ismail W I W, Razak S I A, Razali M H and Amin K A M 2018 Accelerated wound healing of physically cross linked gellan gum-virgin coconut oil hydrogel containing manuka honey *ASM Sci. J.* **11** 166–82
- Nangia S, Paul V K, Deorari A K, Sreenivas V, Agarwal R and Chawla D 2015 Topical oil application and trans-epidermal water loss in preterm very low birth weight infants—a randomized trial *J. Trop. Pediatr.* **61** 414–20
- Ndlovu S P, Ngece K, Alven S and Aderibigbe B A 2021 Gelatin-based hybrid scaffolds: promising wound dressings *Polymers* **13** 17
- Neumann P M, Zur B and Ehrenreich Y 1981 Gelatin-based sprayable foam as a skin substitute *J. Biomed. Mater. Res.* **15** 9–18
- Öztopalan D F, Işık R and Durmuş A S 2017 Yara iyileşmesinde büyüme faktörleri ve sitokinlerin rolü *Dicle Univ. Vet. Fak. Derg.* **10** 83–88
- Park E, Lee S M, Jung I-K, Lim Y and Kim J-H 2011 Effects of genistein on early-stage cutaneous wound healing *Biochem. Biophys. Res. Commun.* **410** 514–9
- Parvez S, Rahman M M, Khan M A, Khan M A H, Islam J M M, Ahmed M, Rahman M F and Ahmed B 2012 Preparation and characterization of artificial skin using chitosan and gelatin composites for potential biomedical application *Polym. Bull.* **69** 715–31
- Pawde S M and Deshmukh K 2008 Characterization of polyvinyl alcohol/gelatin blend hydrogel films for biomedical applications *J. Appl. Polym. Sci.* **109** 3431–7
- Peedikayil F C, Remy V, John S, Chandru T P, Sreenivasan P and Bijapur G A 2016 Comparison of antibacterial efficacy of coconut oil and chlorhexidine on *Streptococcus mutans*: an *in vivo* study *J. Int. Soc. Prev. Community Dent.* **6** 447
- Qadir A, Jahan S, Aqil M, Warsi M H, Alhakamy N A, Alfaleh M A, Khan N and Ali A 2021 Phytochemical-based nano-pharmacotherapeutics for management of burn wound healing *Gels* **7** 209
- Rajpaul K 2015 Biofilm in wound care *Br. J. Community Nurs.* **20** S6–11
- Rohman A, Che Man Y B, Ismail A and Hashim P 2010 Application of FTIR spectroscopy for the determination of virgin coconut oil in binary mixtures with olive oil and palm oil *J. Am. Oil Chem. Soc.* **87** 601–6
- Seleem D, Chen E, Benso B, Pardi V and Murata R M 2016 *In vitro* evaluation of antifungal activity of monolaurin against *Candida albicans* biofilms *PeerJ* **4** e2148
- Sezer A D and Cevher E 2011 Biopolymers as wound healing materials: challenges and new strategies *Biomaterials Applications for Nanomedicine* ed R Pignatello (Rijeka: IntechOpen) pp 383–414
- Shilling M, Matt L, Rubin E, Visitacion M P, Haller N A, Grey S F and Woolverton C J 2013 Antimicrobial effects of virgin coconut oil and its medium-chain fatty acids on *Clostridium difficile* *J. Med. Food* **16** 1079–85
- Sierra-Sánchez Á *et al* 2020 Hyaluronic acid biomaterial for human tissue-engineered skin substitutes: preclinical comparative *in vivo* study of wound healing *J. Eur. Acad. Dermatol. Venereol.* **34** 2414–27
- Ślota D, Florkiewicz W, Piętak K, Szwed A, Włodarczyk M, Siwińska M, Rudnicka K and Sobczak-Kupiec A 2021 Preparation, characterization, and biocompatibility assessment of polymer-ceramic composites loaded with *Salvia officinalis* extract *Materials* **14** 6000
- Sobral P J A, Menegalli F, Hubinger M D and Roques M A 2001 Mechanical, water vapor barrier and thermal properties of gelatin based edible films *Food Hydrocoll.* **15** 423–32
- Srivastava Y, Semwal A D, Sajeevkumar V A and Sharma G K 2017 Melting, crystallization and storage stability of virgin coconut oil and its blends by differential scanning calorimetry (DSC) and Fourier transform infrared spectroscopy (FTIR) *J. Food Sci. Technol.* **54** 45–54
- Suleman Ismail Abdalla S, Katas H, Chan J Y, Ganasan P, Azmi F and Fauzi M B 2021 Gelatin hydrogels loaded with lactoferrin-functionalized bio-nanosilver as a potential antibacterial and anti-biofilm dressing for infected wounds: synthesis, characterization, and deciphering of cytotoxicity *Mol. Pharm.* **18** 1956–69
- Taheri P, Jahanmardi R, Koosha M and Abdi S 2020 Physical, mechanical and wound healing properties of chitosan/gelatin blend films containing tannic acid and/or bacterial nanocellulose *Int. J. Biol. Macromol.* **154** 421–32
- Tanase C E and Spiridon I 2014 PLA/chitosan/keratin composites for biomedical applications *Mater. Sci. Eng. C* **40** 242–7
- Tongnuanchan P, Benjakul S and Prodpran T 2014 Structural, morphological and thermal behaviour characterisations of fish gelatin film incorporated with basil and citronella essential oils as affected by surfactants *Food Hydrocoll.* **41** 33–43
- Vanin F M, Sobral P J A, Menegalli F C, Carvalho R A and Habitante A M Q B 2005 Effects of plasticizers and their concentrations on thermal and functional properties of gelatin-based films *Food Hydrocoll.* **19** 899–907
- Varma R K, Kaushal R, Junnarkar A Y, Thomas G P, Naidu M U, Singh P P, Tripathi R M and Shridhar D R 1985 Polysorbate 80: a pharmacological study *Arzneimittel-Forschung* **35** 804–8
- Vaughn A R, Clark A K, Sivamani R K and Shi V Y 2018 Natural oils for skin-barrier repair: ancient compounds now backed by modern science *Am. J. Clin. Dermatol.* **19** 103–17
- Verallo-Rowell V M, Dillague K M and Syah-Tjundawan B S 2008 Novel antibacterial and emollient effects of coconut and virgin olive oils in adult atopic dermatitis *Dermatitis* **19** 308–15
- Vowden K and Vowden P 2017 Wound dressings: principles and practice *Surgery* **35** 489–94
- Walter M N M, Wright K T, Fuller H R, MacNeil S and Johnson W E B 2010 Mesenchymal stem cell-conditioned medium accelerates skin wound healing: an *in vitro* study of fibroblast and keratinocyte scratch assays *Exp. Cell Res.* **316** 1271–81
- Wang H-J, Li M-Q, Liu W, Yao G-D, Xia M-Y, Hayashi T, Fujisaki H, Hattori S, Tashiro S and Onodera S 2016 Gelatin promotes murine fibrosarcoma L929 cell detachment and protects the cells from TNF $\alpha$ -induced cytotoxicity *Connect. Tissue Res.* **57** 262–9
- Wang Y, Zhang W and Yao Q 2021 Copper-based biomaterials for bone and cartilage tissue engineering *J. Orthop. Transl.* **29** 60–71
- Werner S, Krieg T and Smola H 2007 Keratinocyte-fibroblast interactions in wound healing *J. Invest. Dermatol.* **127** 998–1008
- Yeddes W, Djebali K, Wannas W A, Horchani-Naifer K, Hammami M, Younes I and Tounsi M S 2020

- Gelatin-chitosan-pectin films incorporated with rosemary essential oil: optimized formulation using mixture design and response surface methodology *Int. J. Biol. Macromol.* [154 92–103](#)
- Yousefi K, Hamedeyazdan S, Hodaei D, Lotfipour F, Baradaran B, Orangi M and Fathiazad F 2017 An *in vitro* ethnopharmacological study on *Prangos ferulacea*: a wound healing agent *BioImpacts* [7 75–82](#)
- Zaman H U, Islam J M M, Khan M A and Khan R A 2011 Physico-mechanical properties of wound dressing material and its biomedical application *J. Mech. Behav. Biomed. Mater.* [4 1369–75](#)